Intensities and self-broadening coefficients of the strongest water vapour lines in the 2.7 and 6.25μm absorption bands

Journal of Quantitative Spectroscopy & Radiative Transfer 177 (2016) 92–107

Contents lists available at ScienceDirect

Journal of Quantitative Spectroscopy & Radiative Transfer

journal homepage: www.elsevier.com/locate/jqsrt

Intensities and self-broadening coefficients of the strongest water vapour lines in the 2.7 and 6.25 μm absorption bands

Igor V. Ptashnik [a,*], Robert McPheat [b], Oleg L. Polyansky [c,d], Keith P. Shine [e], Kevin M. Smith [b]

[a] Spectroscopy Division, Zuev Institute of Atmospheric Optics, Siberian Branch of the Russain Academy of Science, 1 Akademichesky Av., Tomsk 634055, Russia
[b] RAL Space, Rutherford Appleton Laboratory, Chilton, Didcot, Oxon OX11 OQX, UK
[c] Department of Physics and Astronomy, University College London, Gower Street, London WC1E 6BT, UK
[d] Institute of Applied Physics, Russian Academy of Science, Nizhnii Novgorod 603950, Russia
[e] Department of Meteorology, University of Reading, Earley Gate, Reading RG6 6BB, UK

ARTICLE INFO

Article history:
Received 28 October 2015
Received in revised form
3 February 2016
Accepted 3 February 2016
Available online 12 February 2016

Keywords:
HITRAN database
H_2O line parameters
Spectral line fitting

ABSTRACT

Intensities and self-broadening coefficients are presented for about 460 of the strongest water vapour lines in the spectral regions 1400–1840 cm^{-1} and 3440–3970 cm^{-1} at room temperature, obtained from rather unique measurements using a 5-mm-path-length cell. The retrieved spectral line parameters are compared with those in the HITRAN database ver. 2008 and 2012 and with recent ab-initio calculations. Both the retrieved intensities and half-widths are on average in reasonable agreement with those in HITRAN-2012. Maximum systematic differences do not exceed 4% for intensities (1600 cm^{-1} band) and 7% for self-broadening coefficients (3600 cm^{-1} band). For many lines however significant disagreements were detected with the HITRAN-2012 data, exceeding the average uncertainty of the retrieval. In addition, water vapour line parameters for 5300 cm^{-1} (1.9 μm) band reported by us in 2005 were also compared with HITRAN-2012, and show average differences of 4–5% for both intensities and half-widths.

1. Introduction

The HITRAN database [1] of spectral line parameters is an important resource for many atmospheric and spectroscopic applications. The latest version contains parameters of about 4.4 million spectral lines, and the database is regularly updated with line parameters derived from new measurements and theoretical calculations. Among different gases, water vapour plays one of the most important roles in the Earth's energy balance. Intensities and pressure broadening coefficients of water vapour lines are basic physical parameters required to calculate the Earth's radiation budget and also to interpret remotely-sensed data.

There is also another related aspect for robust understanding of line parameters. During investigations of water vapour continuum absorption within three near-IR water vapour absorption bands [2–4] the authors identified a requirement for improved knowledge of the intensities and self-broadening coefficients of the strongest water vapour lines within these bands, to achieve a more confident retrieval of the continuum strength. As a result, at first, the parameters of about 450 of the strongest water vapour lines (intensity $S \geq 2 \times 10^{-23}$ cm molec^{-1}) in the 1.9 μm (5000–5600 cm^{-1}) band were derived from thorough fitting [5,6] to the measured high-resolution Fourier transform spectrometer (FTS) spectra, obtained in the Molecular Spectroscopy Facility, Rutherford Appleton

* Corresponding author.
E-mail address: piv@iao.ru (I.V. Ptashnik).

http://dx.doi.org/10.1016/j.jqsrt.2016.02.001

Laboratory (MSF RAL). Comparison of the retrieved in [5,6] self-broadening coefficients with those in the HITRAN-2004 and 2008 [7,8] databases revealed strong (up to 20%) systematic differences for the group of "medium-intensity" lines (from 1×10^{-21} to ca. 6×10^{-21} cm molec^{-1}) with strong evidence in favour of the new data.

The problem with experimental determination of the self-broadening coefficients for the strongest spectral lines lies in saturation of their absorption even at small (a few cm) path-lengths. "Saturation" is considered here as optical depths exceeding 4–5, at which the output signal in FTS measurements becomes comparable with the noise level. Reducing the water vapour pressure can help if one is interested only in determining intensities of these strong lines, as intensity does not depend on line shape. However, it will not help in deriving their self-broadening coefficients, because at small (less than a few millibars) pressures the line shape of water vapour lines in near-IR region at room-temperatures approaches Gaussian with Doppler halfwidth. This would make retrieval of the self-broadening coefficient very uncertain. That is why a very short path length is required in order to keep the pressure not less than a few millibars and still avoid saturation in absorption of these strong water vapour lines.

In the measurements within the 1.9 μm band [5] an absorption cell with a path length of 29.13 cm was used. In the present paper we extend the spectral region to the much stronger water vapour absorption bands 2.7 and 6.25 μm (3600 and 1600 cm^{-1} respectively). Only by reducing the path length to around 5 mm is it possible to reliably measure these lines.

2. Experimental setup

Because of the high absorption cross-section of water vapour lines within the bands under investigation, a special new single-pass cell was constructed at the Rutherford-Appleton Laboratory for these measurements. The cell had a 4.78 mm path length (measured with a micrometer) and was constructed of electropolished stainless steel with Parylene coated KBr windows, attached with low vapour pressure epoxy resin. A 1 litre spherical reservoir volume, attached to the cell, was used to increase the volume-to-surface ratio and stabilise the water vapour pressure (see Fig. 1).

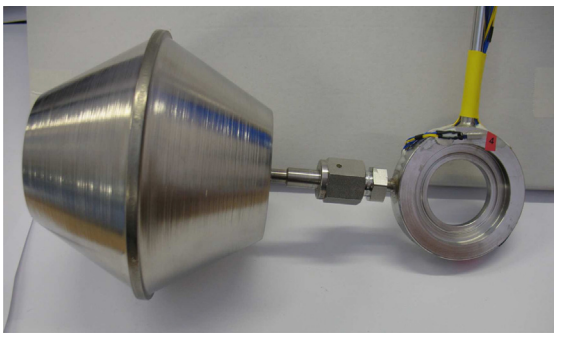

Fig. 1. The 4.78 mm cell with reservoir volume.

The spectra were recorded using an IFS120 which has been upgraded to IFS125 specification (electronics, scan motor and optical layout), but retains the original analogue detectors. The unapodized spectral resolution was 0.002 cm^{-1} (resolution is defined here as 0.9/maximum-optical-path-difference). The Bruker (FTS) was configured with a Globar source. Mertz phase correction [9] was applied to the measured interferograms. An optical filter was used for 6.25 μm band to limit the optical bandwidth to the spectral range of the measurement.

The cell was filled with water vapour to approximately the desired pressure and allowed to reach equilibrium over a period of several hours. The pressure was measured using 2 MKS Baratrons type 670 (1.3 and 13 mbar full scale) and the temperature measured using 4 PRTs attached to the cell. Measurement of spectra commenced when the pressure had stabilised which typically took 12 h in the mid-IR.

The measurements reported here were performed at a temperature about 294 K and at two pure water vapour pressures for the each band, ranging from 5.9 to 13.0 mbar (see the Table 1). Samples of water vapour were prepared using a clean stainless steel vacuum line from distilled liquid water (Analar grade, BDH Chemicals), which had previously been purified to remove dissolved air using at least three repeat 200 K freeze-pump-thaw cycles. During the measurements, pressure and temperature were recorded at 1-s intervals.

Background spectra with an evacuated cell were recorded before and after each filling of the cell. Prior to taking the background spectrum, high-resolution test measurements were performed to check that water vapour had been removed from the gas cell. In all cases, it was ascertained that the intensities of the strongest water vapour lines were reduced to the peak value of the spectral noise in the corresponding spectral region. Taking the ratio of the sample and averaged background spectra minimised errors in the transmittance or absorbance spectra arising from changes in baseline signal level, for example due to drifts in the intensity of the source. Typical background and sample spectra for two water vapour absorption bands investigated in this work are shown in Fig. 2.

The signal-to-noise ratio in each transmittance spectra exceeded 1000:1 across the entire spectral range considered here, giving an information-to-noise ratio in excess of 100:1 for absorbances between 0.2 and 3.5. For

Table 1
Experimental details.

Spectral region	1250–2000 cm^{-1}	1800–6000 cm^{-1}
Source	Globar	Globar
Beamsplitter	KBr	CaF_2
Detector	MCT	InSb
Optical filter	2000 cm^{-1} long wave pass	None
Resolution	0.002 cm^{-1}	0.002 cm^{-1}
Temperature	294 K	294.3 K
Pressures/mbar	7.72, 12.9	5.92, 13.0

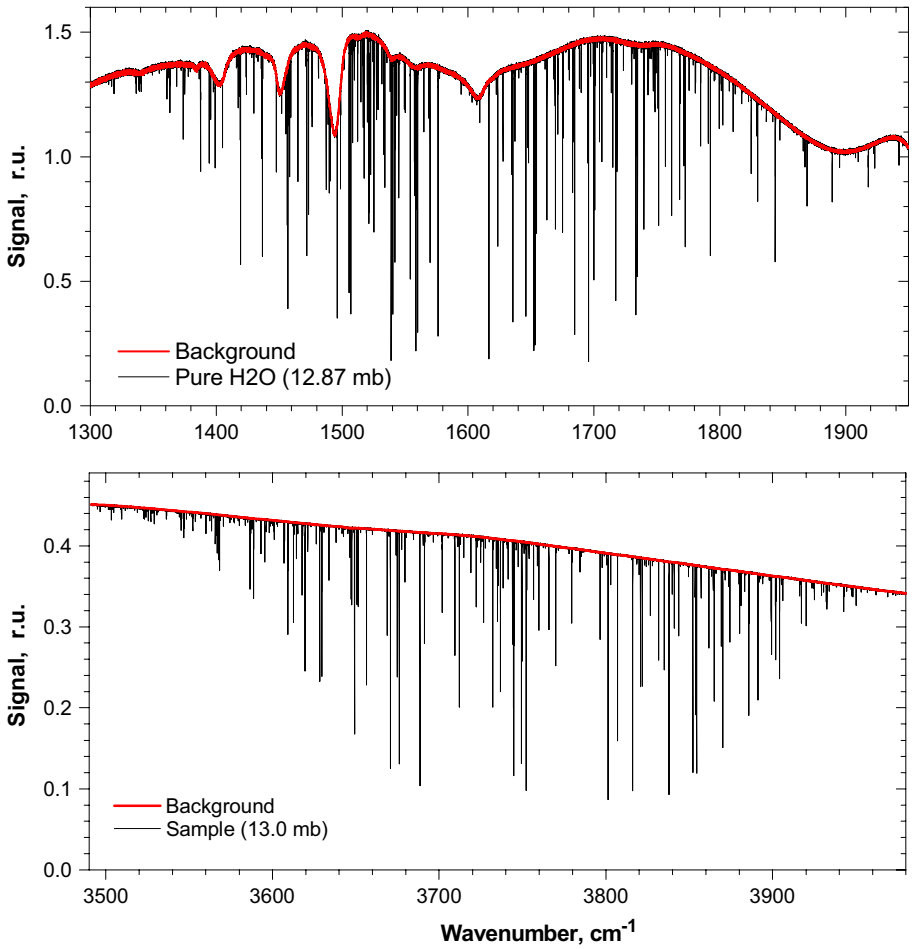

Fig. 2. Example of background (empty cell) and sample (pure water vapour) FTS signal from the 4.78 mm absorption cell at 284 K in the spectral region of 2.7 and 6.25 μm absorption bands.

the 2.7 μm region maximum information-to-noise ratio at an absorbance of about 1.0 was 700:1. The main experimental details are shown in the Table 1.

3. Line fitting

The fitting procedure was similar to that described in detail in [5]. The observed laboratory transmittance spectra were compared with calculated spectra, generated for the measured laboratory conditions, using the HITRAN-2012 [1] water vapour line parameters and the line-by-line code of Mitsel et al. [10]. Information about the optical configuration of the FTS was used to calculate an instrument line shape (ILS) and convolute it with the calculated molecular spectrum. The initial ILS was determined from the ideal 'sinc'-function which was convolved with a boxcar field-of-view (FOV) function to account for the finite FOV of the spectrometer (i.e. the effect of off-axis rays passing through the aperture) [11]. This leads to the broadening of the final ILS function and a shift to lower wavenumber by an amount equal to the half-width of the FOV function.

During the fitting procedure only those parts of the spectrum with an optical depth of less than 4.0 were used, to minimise the impact of saturated spectral intervals. Unapodized FTS spectra were used for the fitting in this work. The undamped ringing (sidelobes) inherent in unapodized ILS functions necessitates the use of far ILS wings to convolve with the simulated spectrum which increases the time taken by the fitting procedure. The optimal distance at which the ILS can be truncated without significant loss in the accuracy of retrieved line parameters has been derived and checked carefully by fitting to synthetic spectra.

We used the Levenberg–Marquardt least squares algorithm to fit the parameters for about 460 of the strongest lines ($S \geq 2 \times 10^{-21}$ cm molec^{-1}), 200 and 260 in the spectral regions 1400–1840 and 3450–3980 cm^{-1} respectively. Four parameters: line centre position, intensity, self-broadening halfwidth γ_{self} and baseline, were fitted for each spectral line using the Voigt profile in the first stage (with the Doppler halfwidth calculated for each line). Then a fifth, the narrowing parameter β, was added to the fitting procedure to account for the collisional narrowing effect (Dicke-effect). The Rautian–Sobelman (R–S) profile

describing a strong collision model [12] was used in a second stage of the fitting procedure. The average value of the pressure independent dimensionless collisional narrowing parameter β/γ_{self} was found to be about 0.3 (with standard deviation 0.35) and 0.17 (standard deviation 0.19) for the 1600 and 3600 cm^{-1} band respectively. It weakly affected the retrieved line intensities and self-broadening coefficients of most lines. Not accounting for the collisional narrowing (i.e., fitting with the Voigt profile) led, on average, to underestimation of the fitted line intensities and self-broadening widths by about 0.5–1.5% and 2–4% respectively.

This work was performed prior to the IUPAC recommendation [13] to use the Hartmann–Tran (H–T) profile [14] for atmospheric applications, and even before papers on this profile were published. It is known however [15] that in the case of dipole-dipole intermolecular interaction, which is dominant for H_2O self-broadening, the relaxation constants should not depend on speed. This should significantly reduce the impact of speed-dependence effect on water vapour lines. Indeed, according to Fig. 1 in [13] using just the Nelkin–Ghatak profile [16] (which accounts for collisional narrowing and is essentially equivalent to the R–S profile) is enough to reduce residuals by a factor of 5 compared to the Voigt profile and to bring deviations from the experimental profile to less than 0.2%. Using the more sophisticated H–T profile, which accounts also for speed-dependence of the relaxation rates and its correlation with velocity change due to collisions, reduces the deviations to below the 0.1% level.

Line-mixing has also rather little effect for H_2O lines at such low pressures. It may slightly affect only particular pairs of water vapour lines, changing derived parameters by 2–4% [17]. Thus, one can expect that for majority of H_2O lines the difference in retrieved intensities and self-broadening coefficients between using the R–S and any more sophisticated line profile should be less than 1%. This is several times less than total experimental uncertainty of our data and thus can be neglected in this work.

The first guesses for each of the line parameters in the fitting procedure were taken from the HITRAN-2008 database. Spectral lines were fitted simultaneously in sets of 5–10 lines. The fitting procedure for the whole spectral region was repeated several times until the total residual between two consecutive iterations became negligible. Every line was fitted within $10\gamma_v$ spectral interval from the line centre, where γ_v is an average Voigt half-width at half-maximum of the spectral line for the measurement ($\gamma_v \sim 0.006$ cm^{-1}). The impact of unfitted spectral lines ($S < 2\times10^{-21}$ cm $molec^{-1}$) was taken into account using parameters from HITRAN-2012.

The final parameters were defined as an average between values derived at two different pressures (see Table 1). Half of the difference between these values was included in the error estimation for the final parameter for every line. The retrieval error for each parameter also includes fitting error (produced by 'DRNLIN' and 'DRSTAT' MS Fortran Library) and uncertainty in the measured water vapour pressure. The latter was estimated in this work as $\approx 2\%$.

The HITRAN-2012-format files with the line parameters converted to the temperature $T_2 = 296$ K is attached as Supplementary material. The parameters were converted according to the usual relations:

$$S(T_2) = S(T_1)(T_1/T_2)^{3/2}\exp\{-E''(hc/k)(1/T_2 - 1/T_1)\};$$

$$\gamma^o{}_{self}(T_2) = (T_1/T_2)^n \gamma^o{}_{self}(T_1);$$

where E'' is the lower state energy of the transition in cm^{-1}; n is the line width temperature dependence, T_1 is the temperature at which the experimental data were obtained. The $S(T_1)$ and $S(T_2)$ are both in cm $molec^{-1}$ here. Information about the intensity and self-broadening errors from this work has also been included in the HITRAN-format file using the HITRAN uncertainty indices.

4. Results and comparison

4.1. 1400–1840 cm^{-1} (δ-band)

Fig. 3 compares intensities (a) and self-broadening coefficients (b) of the water vapour lines derived from fitting to the experimental data in 1400–1840 cm^{-1} spectral region (δ-band) with parameters from HITRAN-2008 [8], 2012 [1] and with the recent results of ab initio calculations by Polyansky et al. [18] (scaled by the isotopologue abundance). These calculations are based on the variational calculations using the DVR3D program suite [19]. As an input for this program the accurate dipole moment surface (DMS) and potential energy surface (PES) of water monomer is necessary. High accuracy ab initio calculation of the DMS is presented in [20], while semi-empirical PES of high accuracy is given in [21]. The details of the calculation of the linelist with the line centres and line intensities used in this work will be presented in a forthcoming paper [18]. The line intensities calculated using Lody et al.'s DMS [20] have been compared with the experimental measurements of intensities of sub-percent accuracy made by Lisak et al. [22] in the spectral region of 7200 cm^{-1}, and very recent comparison with the intensities [18] in the region of 3600 cm^{-1} of water fundamental bands has been made by Pogany et al. [23]. In both cases the discrepancy within experimental error has been demonstrated: less than 1% for the data around 7200 cm^{-1} [22] and about 2% for the fundamental bands in [23]. These comparisons suggest that we might expect the accuracy of the intensity calculations of water absorption lines [20] to be within about 2%. The preliminary results of Polyansky et al. [18] calculations for intensities of some strongest H_2O lines are tabulated in the Supplementary file.

Comparison shows that intensities of the strongest H_2O lines in HITRAN-2012 [1], originating from semi-empirical calculations by Coudert et al. [27,28], appear systematically underestimated (by 3.4%) compared to the result of our fitting. The situation is a little better than for the HITRAN-2008 (4.2% deviation). This deviation lies slightly beyond the error-bars of our experimental data. However, comparison with the calculations of Polyansky et al. [18]

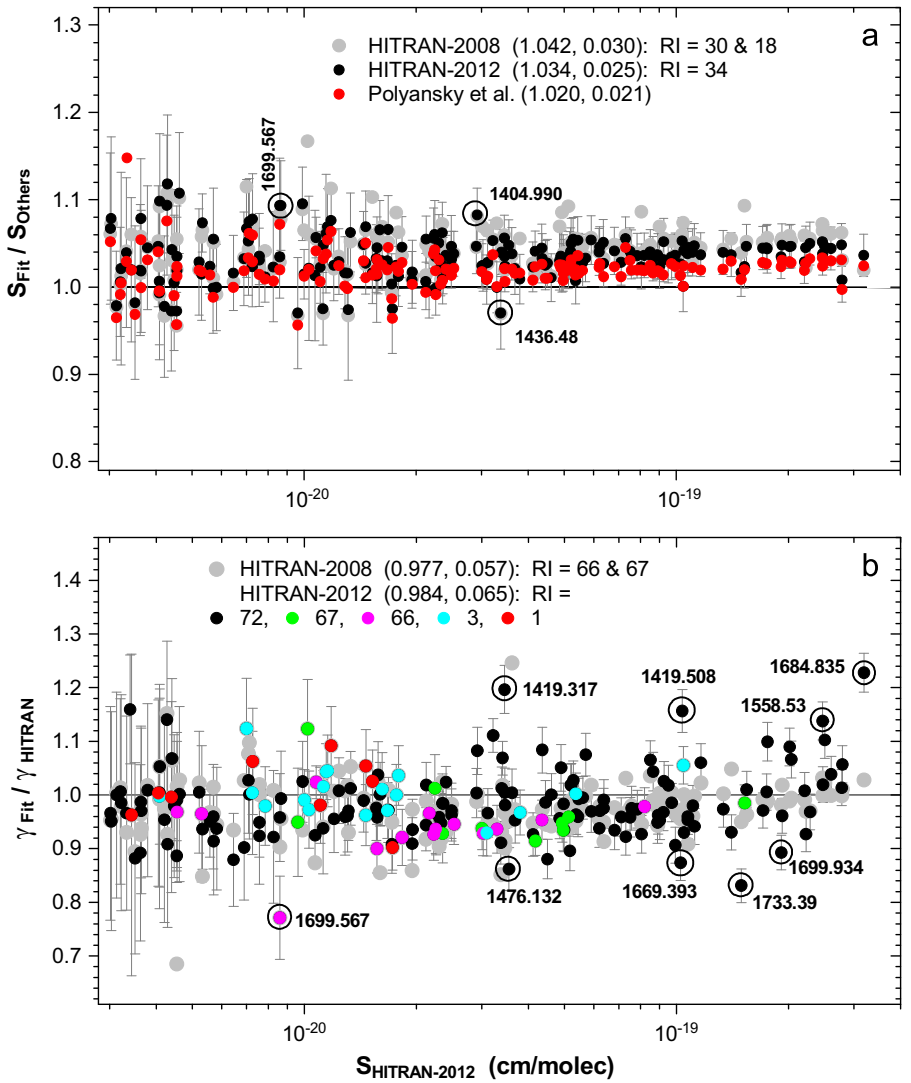

Fig. 3. Ratio of water vapour line intensities (a) and self-broadening coefficients (b), obtained in this work by fitting to the experimental data in the spectral region 1400–1840 cm^{-1}, to corresponding parameters in HITRAN-2008 [8], HITRAN-2012 [1] and ab initio calculations by Polyansky et al. [18]. Numbers in parentheses show mean value and standard deviation. For one set of data the uncertainty in the retrieved parameters are shown by error-bars. The circled datapoints correspond to absorption lines shown in Fig. 4 with wavenumbers (cm^{-1}) stated nearby. The 'RI' refers to the Reference Indices used in HITRAN for particular sets of line parameters as following: 1 – 'For perpendicular bands derived from' Toth et al. [24], 'for parallel bands from Toth, JPL, unpublished'; 3 – Toth [25]; 18 – Toth [26]; 30 – Coudert et al. [27]; 34 – semi-empirical calculations by Coudert et al. [27,28]; 66 – Gamache and Hartmann [29]; 67 – Antony and Gamache [30]; 72 – Birk and Wagner [31].

demonstrates a much better agreement with our values of intensities with systematic deviation of only 2.0%.

By contrast with the intensities, self-broadening coefficients (Fig. 3b) of the strongest (above 10^{-19} cm/molec) lines in HITRAN-2012 demonstrate markedly wider disagreement with our experimental values than, on average, those in the older (HITRAN-2008) version, reaching 15–20% for some lines. Analysis of the HITRAN reference indices presented in Fig. 3b, points to the reference index '72' as the source of self-broadening parameters in HITRAN-2012 having the largest deviation from our experimental data. The reference index '72' corresponds to the high-quality FTS measurements by Birk and Wagner [31]. It corresponds either to the values directly measured by Birk and Wagner [31] (for the lines with intensity less than $\sim 5 \cdot 10^{-21}$ cm/molec)[1] or are transferred (for stronger lines) from weaker transitions with the same upper and lower rotational quantum numbers (neglecting

[1] The minimal absorption path length used in [31] was about 25 cm. This means that the most intense water vapour lines were either critically saturated under pure self-broadening conditions in the experiments of [31] or strongly dominated by foreign broadening when a mixture with air was used. That is perhaps the reason why Table 5 in [31] (where the authors presented only high-accuracy derived parameters) does not contain self-broadening values for lines with intensities $\geq 5 \times 10^{-21}$ cm/molec. This was not the case in our experiment, which was specially designed for measuring the strongest self-broadened water vapour lines using the ultra-short absorption cell.

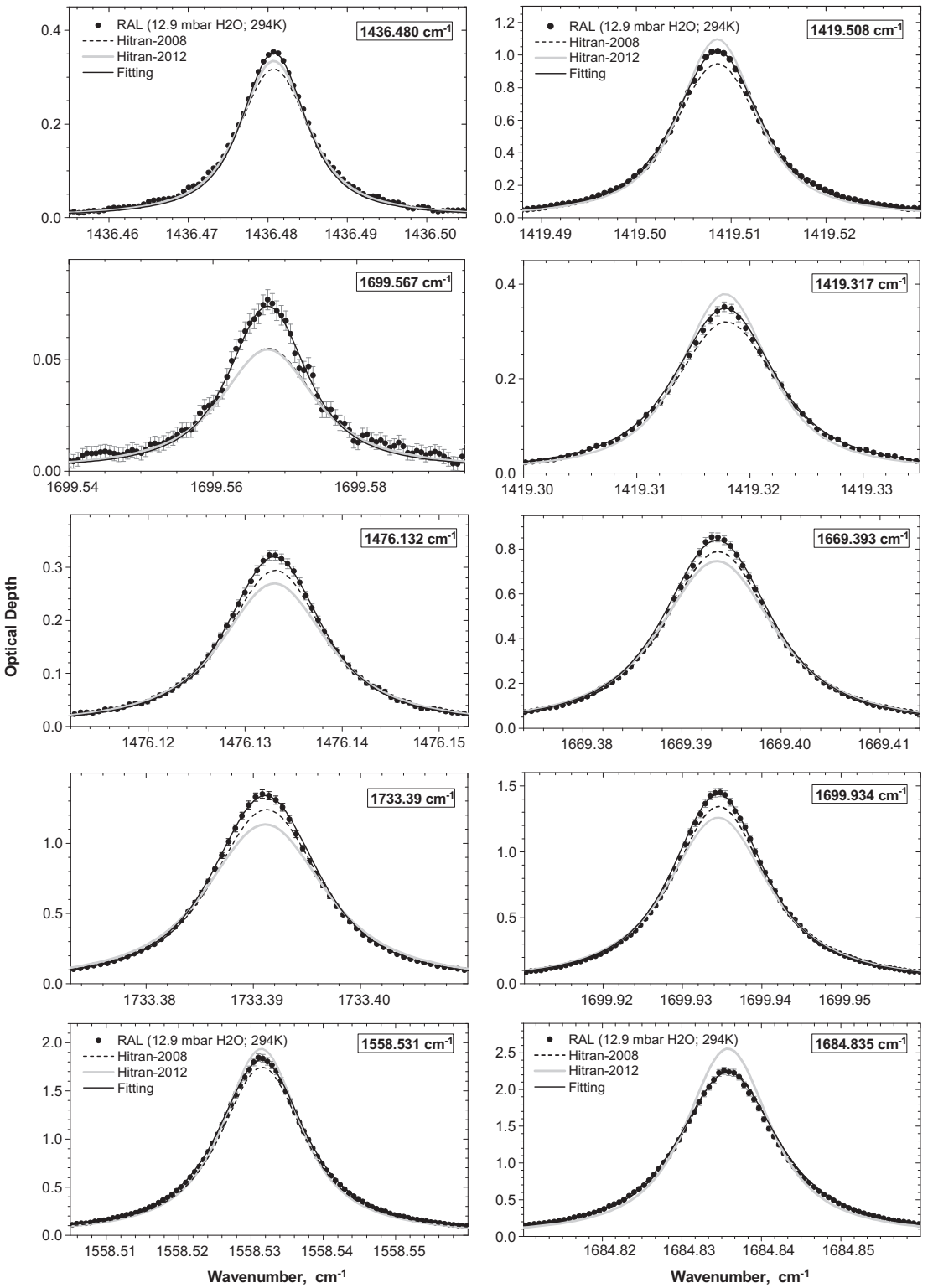

Fig. 4. Comparison of the measured spectra and calculated ones using line parameters from the two different HITRAN versions and parameters derived in this work by fitting to the new experimental data. The eight lines marked in Fig. 3 are shown. The measured spectra were obtained in pure water vapour at 12.9 mbar, path length 4.78 mm and at a temperature of 294 K.

vibrational dependence in this region). Unfortunately it appears that in a few cases the data was not transferred from Birk and Wagner [31] paper to HITRAN correctly (Iouli Gordon, pers. comm.). For instance, self-broadening of the 1684.835 cm^{-1} line in HITRAN ((010)-(000) (4,1,4)-(3,0,3) in the notation (V')-(V") (J',Ka',Kc')-(J",Ka",Kc"'); see also Fig. 3), was supposed to be taken from the corresponding measurement [31] of the line with same rotational quanta, but in a hot band ((020)-(010) (4,1,4)-(3,0,3)). However, the value for both transitions in HITRAN appears to be 0.416 cm^{-1}/atm, while Table 5 of Ref. [31] gives 0.5167 cm^{-1}/atm which is in excellent accord with the value of 0.511 cm^{-1}/atm that we measured.

Fig. 4 shows a few examples of comparison of experimental and simulated spectra for several lines having significant deviation from the HITRAN-2012 parameters in this band and highlighted in Fig. 3. It can be seen that fitting the procedure reproduces the experimental spectrum rather well. Visual verification of the fitting accuracy was performed for all lines for which parameters indicate a significant deviation from HITRAN-2012.

4.2. 3440–3970 cm^{-1} (ν-polyad)

Figs. 5–7 show similar comparison for line parameters derived from fitting in 3440–3970 cm^{-1} spectral region

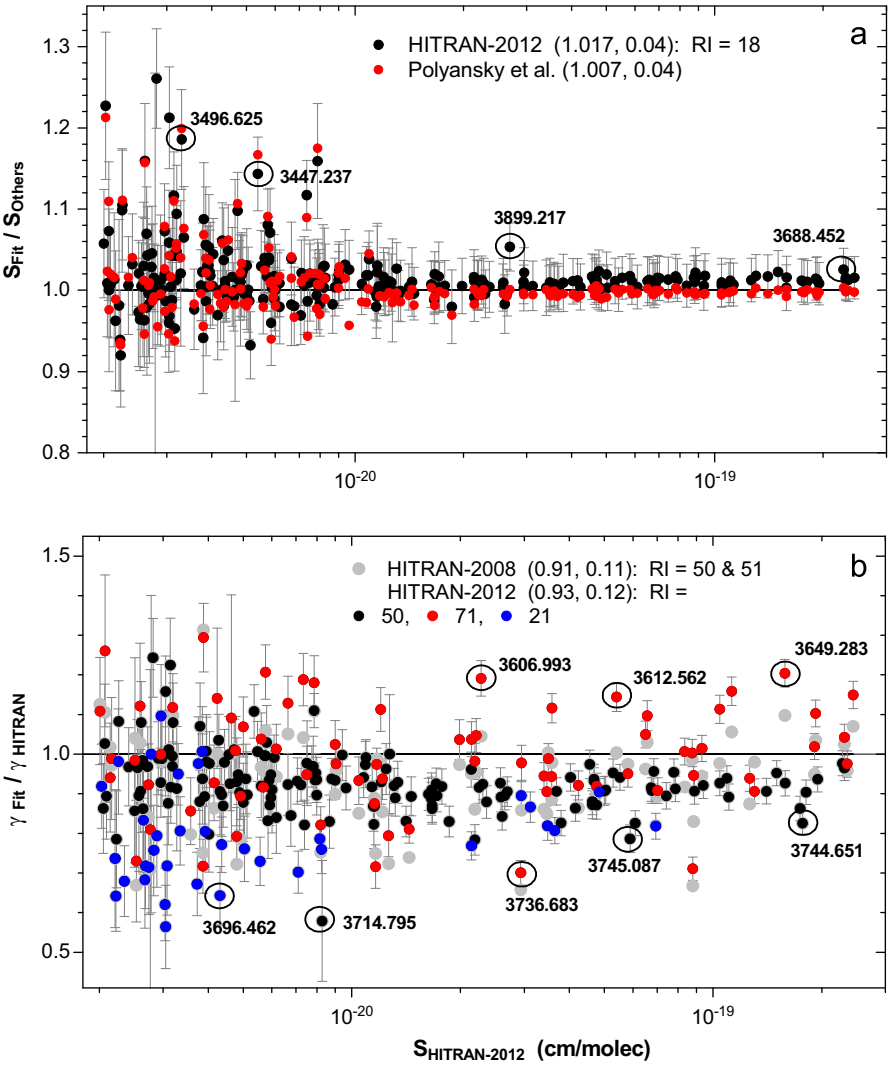

Fig. 5. Ratio of water vapour line intensities (a) and self-broadening coefficients (b), obtained in this work by fitting to experimental data in spectral region 3440–3970 cm^{-1} (ν-polyad), to corresponding parameters in HITRAN-2012 [1] and ab initio calculations by Polyansky et al. [18]. Numbers in parentheses are the mean value and standard deviation. For one set of data the uncertainty in the retrieved parameters are shown by error-bars. The circled data points correspond to absorption lines shown in Figs. 6 and 7 with wavenumbers (cm^{-1}) stated nearby. The 'RI' refers to the Reference Indices used in HITRAN for particular sets of line parameters as following: 18 – Toth [26]; 21 – Mandin et al. [32]; 50 – smoothed values from Toth [25]; 51 – 'R.R. Gamache, unpublished data, average values of experimental data as a function of J'' (2000)'; 71 – Polynomial fit of the values from [30], averaged as a function of J" and asymptotic value of γ_{self} (J"=50)=0.0400 $cm^{-1}atm^{-1}$ (see [33] for details).

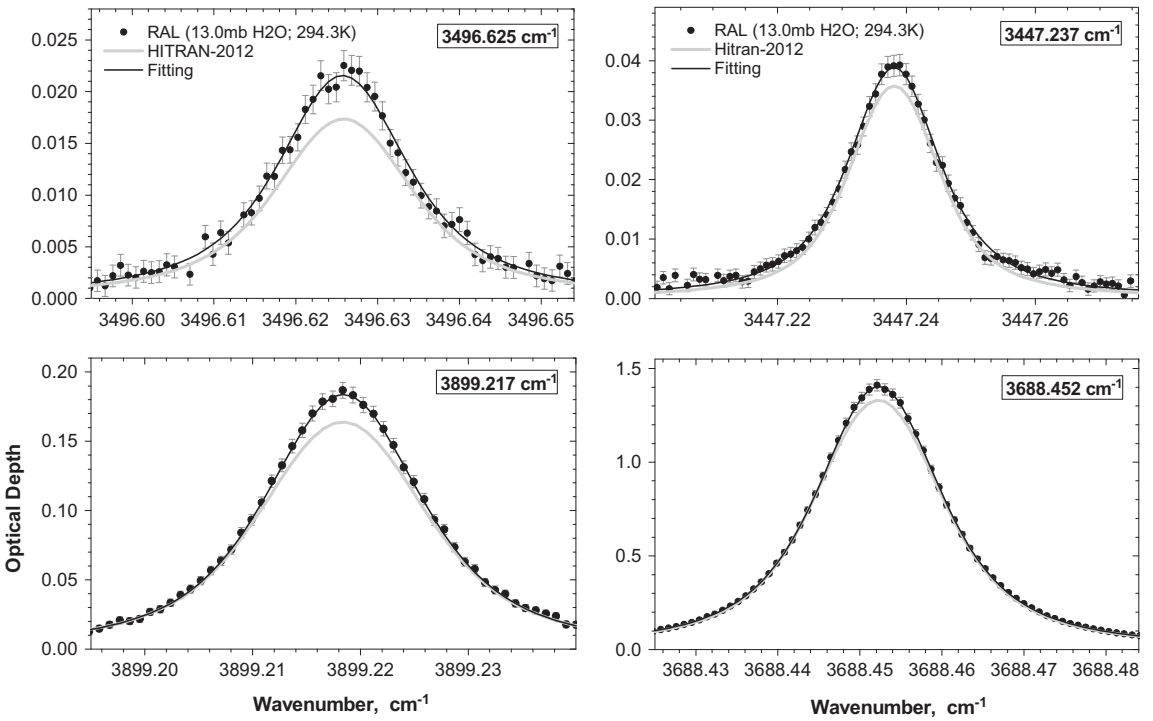

Fig. 6. Comparison of the measured spectra with calculated ones using line parameters from HITRAN-2012 [1] and parameters derived in this work by fitting to the new experimental data. Four lines highlighted in Fig. 5a are shown. The measured spectra were obtained in pure water vapour at 13 mbar, path length 4.78 mm and at a temperature of 294.3 K.

(ν-polyad). The HITRAN-2008 [8] and 2012 [1] versions have the same source for H_2O line intensities in for this polyad (R.A. Toth, Linelist of water vapour parameters from 500 to 8000 cm^{-1}, http://mark4sun.jpl.nasa.gov/h2o.html), and so only comparison with HITRAN-2012 is presented. Although the average deviation between fitted line intensities and those in HITRAN-2012 is rather small (1.7%) and lies within the uncertainty of the retrieved values, the values produced by calculations [18] are in almost perfect agreement with our experimental values for intensities above 1×10^{-20} cm/molec. Again, visual comparison of the experimental and calculated (using fitted parameters) spectra demonstrates the very good quality of the fitting procedure (Figs. 6 and 7). It also shows that the HITRAN-2012 self-broadening coefficients of many strong water vapour lines in this spectral region should be corrected. The main source of disagreement comes from lines with the HITRAN reference (code '71') that refers to 'polynomial fit of the values from' [30], citing also [33] for details. The 'smoothed values from Toth' [25] (reference code '50') show a systematic overestimation by about 7% compared to our data.

4.3. 5040–5580 cm^{-1} ($\nu+\delta$ polyad)

In previous papers [5,6] we reported new line parameters in ($\nu+\delta$ polyad) derived using a short-path (29.13 cm) absorption cell and compared these with previous versions of HITRAN data. Figs. 8 and 9 here show comparison of our data [6] with HITRAN-2012. As can be seen, there are not any substantial differences between line intensities in HITRAN-2008 and HITRAN-2012. The mean systematic deviation from our experimental values is about 5% and lies just within the uncertainty of the experimental data. The main source of the values in HITRAN-2012 are calculations by Lodi et al. [20]. These values are also in good agreement with the result of Polyansky et al. calculations [18], which is not surprising, taking into account that both calculations utilised the same dipole moment surface. It is interesting to note that our experimental data have, on average, a zero systematic deviation from intensity values in the HITRAN-2001 update (v. 11) [35] (see Fig. 8a and also [5]), where the main set of line intensities in this polyad was provided from the experimental data of Toth. It is important to mention that in [5] this fact was verified also by comparison with intensities derived from fitting to independently measured air-broadened water vapour spectrum. This makes us suggest that ab-initio calculations [18,20] may still systematically overestimate the intensities of the strongest lines in this spectral region by ca. 3–4%. Additional independent measurements are required to investigate this further.

The strong sawtooth-like deviation in self-broadening coefficients from our experimental data, that was reported earlier [5,6] for the HITRAN-2004 and 2008 versions, was corrected in HITRAN-2012 (Fig. 8b). However, the mean value of the remaining systematic deviation and the spread is still quite large, and the self-broadening coefficients of many lines in this spectral region require correction (see Figs. 8b and 9).

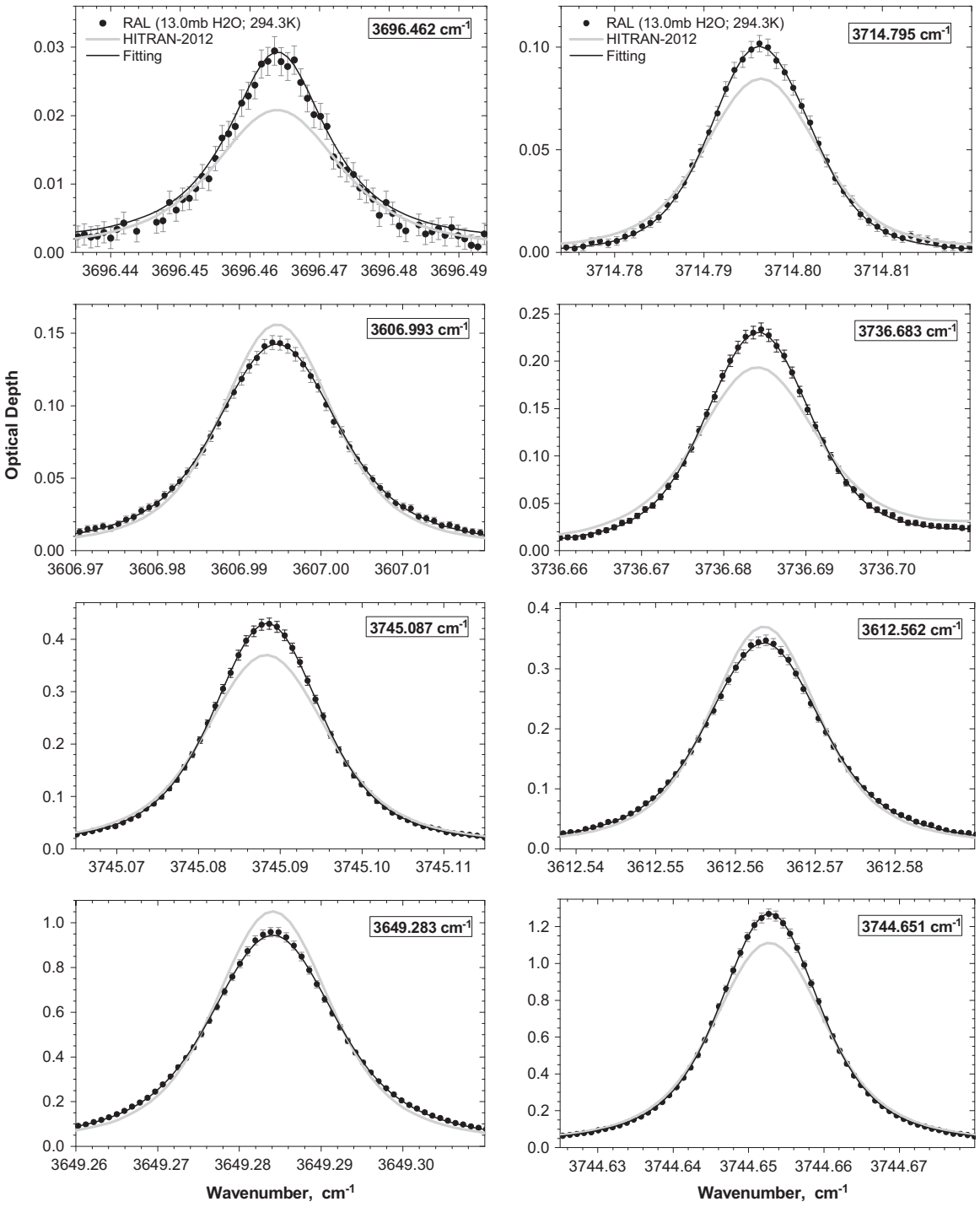

Fig. 7. A similar comparison as in Fig. 6, but for lines highlighted in Fig. 5b as those having significant deviations from HITRAN-2012 in terms of the self-broadening parameter.

5. Conclusion

We have presented intensities and self-broadening coefficients of about 460 of the strongest water vapour lines in the spectral regions 1400–1840 cm^{-1} and 3440–3970 cm^{-1} at room temperature, obtained from rather unique FTS measurements using a 5-mm-path-length cell, which avoids saturation of these strong lines and retains

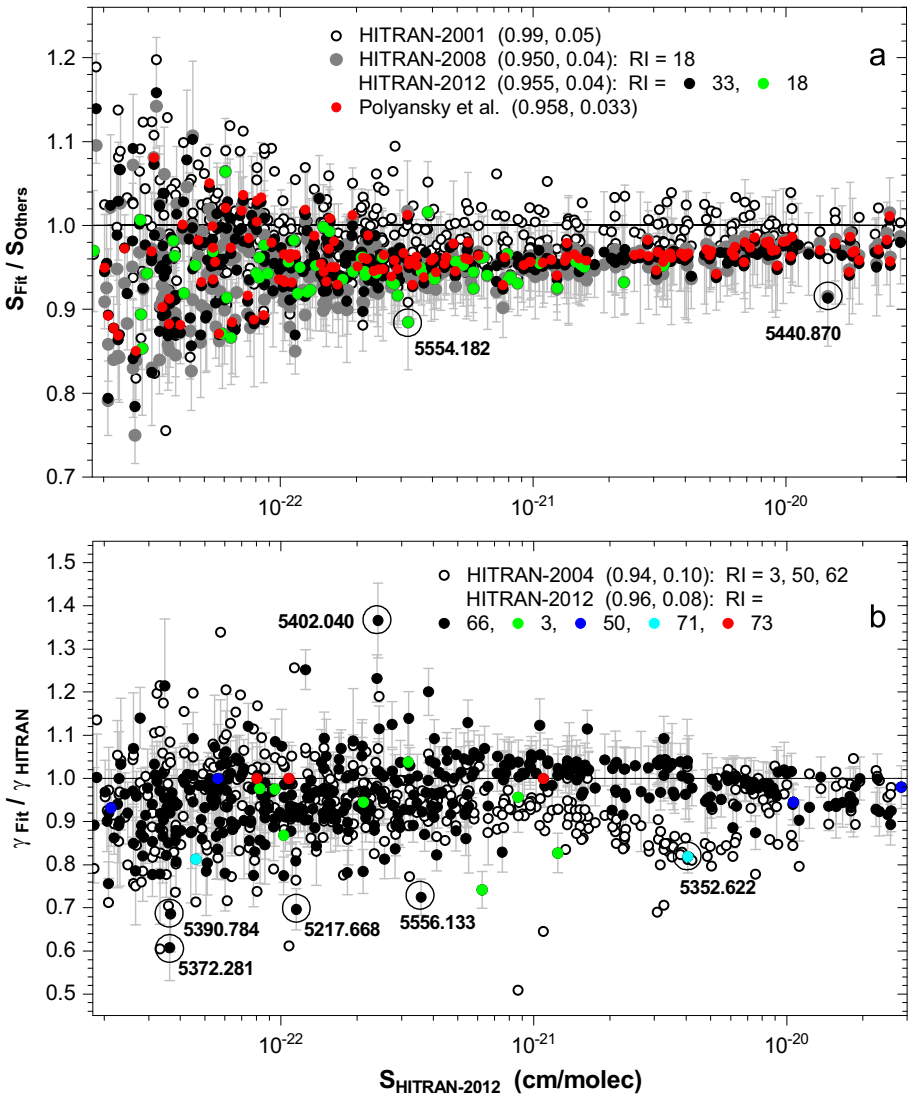

Fig. 8. Ratio of water vapour line intensities (a) and self-broadening coefficients (b), obtained by Ptashnik et al. [5] and Ptashnik and Smith [6] from fitting to experimental data in the spectral region 5040–5580 cm^{-1} ($\nu+\delta$ polyad), to corresponding parameters in HITRAN-2001 [35], HITRAN-2004 [7], HITRAN-2012 [1] and Polyansky et al. ab initio calculations [18]. Numbers in parentheses are the mean values and standard deviations. For one set of data the uncertainty in the retrieved parameters are shown by error-bars. The circled datapoints correspond to absorption lines shown in Fig. 9 with wavenumbers (cm^{-1}) stated nearby. The 'RI' refers to the Reference Indices used in HITRAN for particular sets of line parameters as following: 3 – Toth [25]; 18 – Toth [26]; 33 – Lodi et al. [20]; 50 – smoothed values from Toth [25]; 62 – Toth [34]; 66 - Gamache and Hartmann [27]; 71 – Polynomial fit of the values from [30], averaged as a function of J'' and asymptotic value of γ_{self} ($J''=50$)=0.0400 cm^{-1} atm^{-1} (see [33] for details); 73 – [6].

information on the self-broadening. The retrieved spectral line parameters are compared with those in the HITRAN database ver. 2008 and 2012 and with recent ab-initio calculations. Both the retrieved intensities and half-widths are, on average, in reasonable agreement with those in HITRAN-2012. Maximum systematic differences do not exceed 4% for intensities (1600 cm^{-1} band) and 7% for self-broadening coefficients (3600 cm^{-1} band). For many lines, however, significant disagreements were detected with the HITRAN-2012 data, markedly exceeding the average uncertainty of the retrieval (on average 3% for line intensities and 5% for self-broadening coefficients of the strongest lines in the two investigated bands).

In addition, our earlier reported water vapour line parameters for 5300 cm^{-1} (1.9 μm) band were also compared with those in HITRAN-2012. Again, although the systematic deviation lies within 4–5%, still, for many line parameters, especially for the self-broadening coefficients, deviations exceed the uncertainty in our experimental data. Systematic disagreement by 3–4% with the recent ab initio calculations [18,20] for line intensities in this spectral region indicates the need for independent experimental investigation.

Table 2 provides a short list of the newly-derived parameters in the δ and $\nu+\delta$ bands for those lines whose parameters deviate from the HITRAN-2012 values

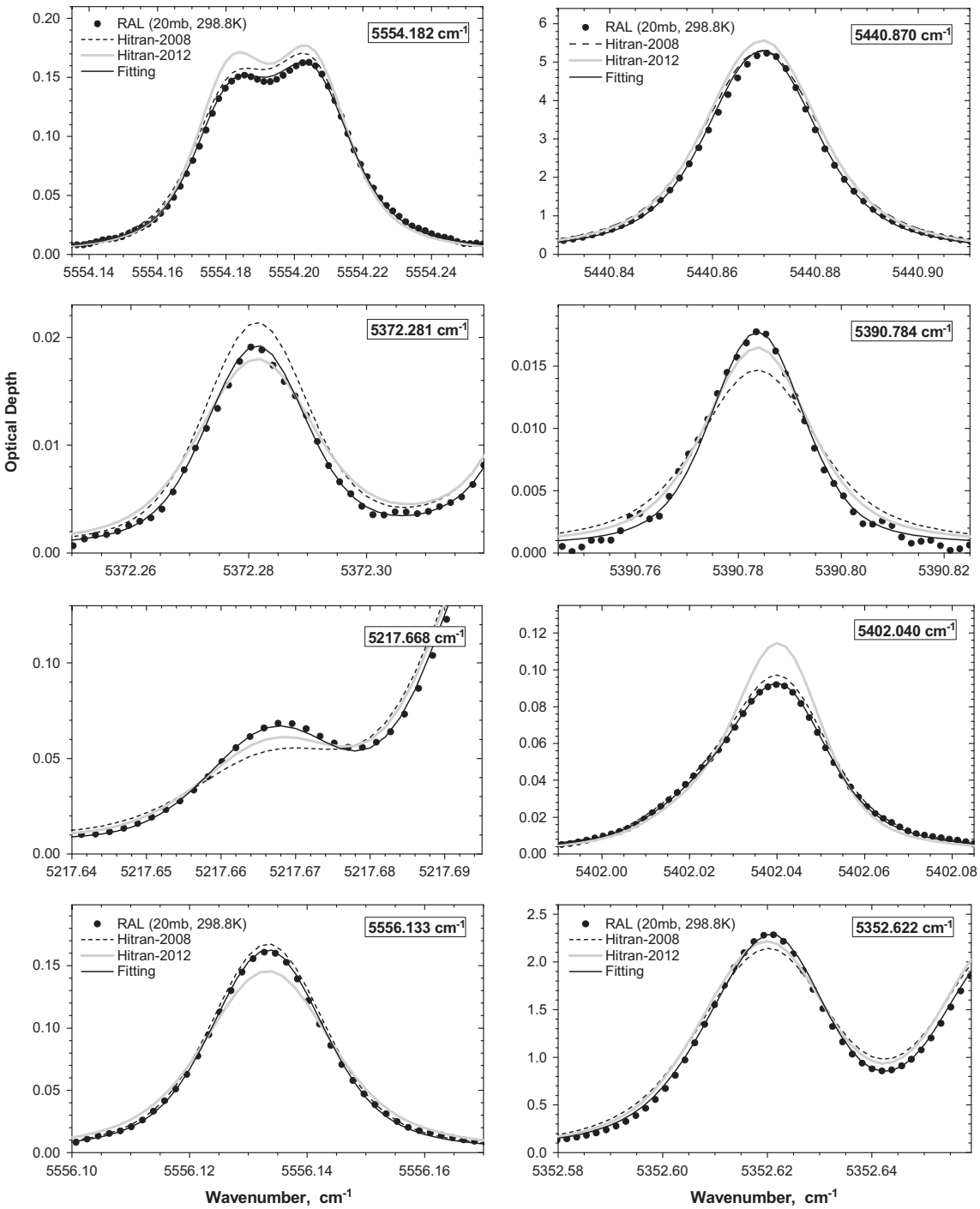

Fig. 9. Comparison of the measured spectra with calculated ones using line parameters from HITRAN-2008, 2012 and parameters derived by fitting to experimental data [5,6] in the spectral region 5040–5580 cm^{-1} ($\nu+\delta$ polyad). Lines highlighted in Fig. 8 are shown. The measured spectra were obtained in pure water vapour at 20 mbar, path length 29.13 cm and at a temperature of 298.8 K.

by more than the error in the derived parameters. The full list of the experimentally derived parameters as compared to the HITRAN-2012 is given in the Supplementary file 'Suppl_Tables'. This file also contains preliminary values of ab initio intensities from Polyansky et al. [18] shown in this work. In two additional supplementary files we also provide the same parameters (derived using both Voigt and Rautian-Sobelman line profile) in the HITRAN format.

Table 2
Intensities S_{fit} and self-broadening coefficients γ^{o}_{fit} of the strongest H_2O lines* within two absorption bands in the 1500–1830 and 3447–3953 cm^{-1} spectral regions, derived in this work by fitting Voigt profile to experimental FTS spectra. All parameters correspond to the temperature of 296 K. Also shown are estimated relative errors δ(%) and ratios of the derived values to those from HITRAN-2012 [1]. Quantum numbers (upper state vibrational index V′, and rotational indices J′, Ka′, Kc′, J″, Ka″, Kc″) and line positions are taken from HITRAN-2012. The lower state vibrational index V″ is ′000′ for all lines.

Wavenumber, cm^{-1}	S_{fit} (cm $molec^{-1}$)	δ (%)	S_{fit}/S [1]	γ^{o}_{fit} (cm^{-1} atm^{-1})	δ (%)	$\gamma^{o}_{fit}/\gamma^{o}$ [1]	V′	J′	Ka′	Kc′	J″	Ka″	Kc″
1404.9900	3.159E-20	4	1.083	0.468	4	1.083	010	5	2	3	6	3	4
1417.2532	5.717E-21	4	1.073	0.280	8	0.937	010	8	0	8	9	1	9
1418.9330	1.965E-20	4	1.008	0.407	5	0.909	010	4	2	2	5	3	3
1419.3172	3.645E-20	3	1.056	0.348	4	1.197	010	3	3	1	4	4	0
1419.5080	1.091E-19	3	1.053	0.354	4	1.157	010	3	3	0	4	4	1
1436.4802	3.277E-20	6	0.970	0.300	4	0.911	010	7	0	7	8	1	8
1436.8182	1.113E-19	3	1.038	0.422	4	0.954	010	3	2	1	4	3	2
1456.5097	6.692E-20	3	1.051	0.359	4	0.976	010	6	1	6	7	0	7
1456.8871	1.833E-19	4	1.044	0.441	3	1.099	010	2	2	1	3	3	0
1458.2670	6.226E-20	4	1.054	0.426	4	0.970	010	2	2	0	3	3	1
1464.9051	9.737E-20	3	1.052	0.478	4	1.026	010	2	1	2	3	2	1
1472.0512	1.171E-19	3	1.047	0.465	3	0.942	010	3	1	2	4	2	3
1473.5142	1.122E-19	4	1.046	0.423	3	0.960	010	5	0	5	6	1	6
1476.1325	3.716E-20	4	1.048	0.393	4	0.862	010	5	1	5	6	0	6
1487.3485	5.359E-20	4	1.036	0.413	4	0.896	010	2	1	1	3	2	2
1489.8419	4.505E-20	4	1.033	0.400	4	1.084	010	6	1	6	6	2	5
1490.8256	5.572E-20	3	1.055	0.458	3	1.027	010	4	0	4	5	1	5
1498.8032	5.894E-20	4	1.033	0.459	4	1.075	010	1	1	1	2	2	0
1505.6042	2.107E-19	3	1.046	0.492	3	1.090	010	1	1	0	2	2	1
1507.0583	2.130E-19	3	1.047	0.513	3	1.066	010	3	0	3	4	1	4
1508.5588	4.547E-20	4	1.045	0.465	4	0.954	010	4	2	3	5	1	4
1512.2105	4.418E-21	3	0.973	0.293	3	0.887	010	7	3	5	7	4	4
1512.3073	4.347E-20	3	1.041	0.377	3	0.915	010	6	2	5	6	3	4
1514.9874	2.491E-20	3	1.036	0.307	3	1.024	010	6	3	4	6	4	3
1516.2933	1.179E-20	3	1.048	0.339	3	1.016	010	5	3	3	5	4	2
1516.7080	3.388E-20	3	1.053	0.339	3	1.111	010	4	3	2	4	4	1
1517.4309	6.520E-20	3	1.046	0.448	3	0.971	010	3	1	3	4	0	4
1517.7828	1.137E-20	3	1.057	0.346	3	1.024	010	4	3	1	4	4	0
1520.1531	3.544E-20	3	1.039	0.361	3	1.069	010	5	3	2	5	4	1
1521.3090	9.221E-20	4	1.037	0.453	4	0.949	010	5	0	5	5	1	4
1525.4994	8.939E-20	3	1.033	0.401	3	1.044	010	4	2	3	4	3	2
1527.3204	3.102E-20	4	1.025	0.427	4	0.928	010	7	1	6	7	2	5
1528.5682	2.621E-20	3	1.038	0.410	4	0.946	010	3	2	2	3	3	1
1533.1823	4.626E-20	4	1.027	0.415	4	0.881	010	3	1	3	3	2	2
1539.0608	2.328E-19	3	1.045	0.445	3	0.927	010	1	0	1	2	1	2
1542.1598	1.206E-19	3	1.037	0.484	3	1.061	010	2	1	2	2	2	1
1549.6417	1.918E-20	5	1.046	0.415	6	0.921	010	6	2	4	6	3	3
1554.3523	1.390E-19	3	1.040	0.448	3	0.974	010	5	1	4	5	2	3
1557.4860	5.734E-20	4	1.054	0.449	4	0.960	010	2	1	1	2	2	0
1557.6092	6.454E-20	3	1.040	0.488	4	0.938	010	0	0	0	1	1	1
1558.5309	2.600E-19	3	1.052	0.497	3	1.138	010	3	0	3	3	1	2
1559.6901	7.097E-20	3	1.041	0.456	4	0.934	010	4	1	3	4	2	2
1560.2571	2.401E-19	3	1.050	0.443	3	0.969	010	3	1	2	3	2	1
1568.9398	2.355E-20	4	1.056	0.476	5	0.926	010	2	2	1	3	1	2
1569.7886	1.091E-19	3	1.042	0.421	4	0.930	010	2	0	2	2	1	1
1616.7115	2.621E-19	3	1.047	0.478	3	1.103	010	1	1	0	1	0	1
1623.5591	9.242E-20	3	1.035	0.424	4	0.962	010	2	1	1	2	0	2
1635.6518	2.015E-19	3	1.048	0.497	3	0.961	010	3	1	2	3	0	3
1645.9693	1.785E-19	3	1.045	0.463	3	0.971	010	3	2	1	3	1	2
1648.3104	4.216E-20	4	1.023	0.419	4	0.926	010	2	2	0	2	1	1
1653.2671	2.722E-19	3	1.044	0.453	3	1.038	010	2	1	2	1	0	1
1662.8093	8.853E-20	3	1.040	0.488	3	1.065	010	2	2	1	2	1	2
1669.3929	1.053E-19	3	1.026	0.417	4	0.874	010	3	1	3	2	0	2
1675.1726	1.029E-19	3	1.036	0.445	4	0.906	010	4	0	4	3	1	3
1683.9836	5.079E-20	4	1.022	0.413	4	0.934	010	5	3	2	5	2	3
1684.8352	3.308E-19	3	1.036	0.511	3	1.228	010	4	1	4	3	0	3
1695.4594	5.067E-20	4	1.035	0.420	4	1.051	010	3	3	0	3	2	1
1697.5272	1.564E-20	5	1.069	0.426	7	1.054	010	5	2	4	5	1	5
1699.5671	9.400E-21	7	1.093	0.427	9	0.771	010	6	1	5	6	0	6
1699.9339	1.980E-19	3	1.035	0.474	3	0.893	010	2	2	1	1	1	0
1700.5007	7.815E-20	3	1.041	0.465	4	0.959	010	5	1	4	4	2	3
1715.1550	7.710E-20	3	1.055	0.410	4	0.922	010	6	0	6	5	1	5
1718.8008	2.334E-20	4	1.035	0.382	5	0.937	010	6	3	4	6	2	5
1733.3905	1.519E-19	4	1.017	0.365	4	0.831	010	7	0	7	6	1	6
1734.3933	5.129E-20	4	1.027	0.369	4	0.935	010	7	1	7	6	0	6
1734.6505	1.457E-19	3	1.037	0.488	3	0.930	010	4	2	3	3	1	2

Table 2 (*continued*)

Wavenumber, cm^{-1}	S_{fit} (cm $molec^{-1}$)	δ (%)	S_{fit}/S [1]	γ^{s}_{fit} (cm^{-1} atm^{-1})	δ (%)	$\gamma^{s}_{fit}/\gamma^{o}$ [1]	V'	J'	Ka′	Kc′	J''	Ka″	Kc″
1743.0504	1.684E-20	7	0.975	0.363	4	0.902	010	5	4	1	5	3	2
1749.4028	1.271E-20	5	1.076	0.402	7	1.092	010	6	4	3	6	3	4
1750.9841	3.076E-20	3	1.024	0.324	4	0.938	010	8	0	8	7	1	7
1751.4233	9.233E-20	3	1.024	0.321	4	0.953	010	8	1	8	7	0	7
1756.8188	5.080E-20	5	1.030	0.390	4	0.948	010	7	1	6	6	2	5
1761.8285	8.238E-20	3	1.023	0.423	4	0.927	010	6	2	5	5	1	4
1837.1809	7.466E-21	7	1.067	0.477	9	1.124	010	7	3	5	6	2	4
–	–	–	–	–	–	–	–	–	–	–	–	–	–
3442.5030	3.698E-21	7	1.212	0.521	8	1.158	100	4	2	3	5	3	2
3447.2370	6.133E-21	5	1.143	0.449	6	1.108	100	3	3	0	4	4	1
3488.0218	3.545E-21	7	1.261	0.444	9	1.243	100	7	0	7	8	1	8
3496.6247	3.913E-21	7	1.186	0.548	8	0.949	100	5	1	4	6	2	5
3503.2758	9.119E-21	8	1.159	0.547	4	1.110	100	2	2	1	3	3	0
3504.7501	3.021E-21	8	1.159	0.506	11	1.079	100	2	2	0	3	3	1
3509.4212	3.496E-21	7	1.094	0.432	10	1.079	001	8	3	5	9	3	6
3518.9919	2.490E-21	10	1.227	0.605	11	0.919	001	4	1	3	5	3	2
3530.7598	2.358E-21	7	1.006	0.391	11	0.679	100	5	1	5	6	0	6
3545.0376	4.002E-21	6	1.030	0.431	8	1.294	001	7	2	5	8	2	6
3557.1296	2.087E-21	8	0.939	0.422	11	0.641	100	1	1	1	2	2	0
3560.1326	8.384E-21	6	1.029	0.355	4	0.786	001	6	4	2	7	4	3
3565.6722	1.342E-20	4	1.027	0.384	4	0.920	001	6	3	3	7	3	4
3566.0804	5.907E-21	5	0.989	0.353	7	0.890	001	7	1	6	8	1	7
3566.7525	1.639E-20	4	0.989	0.320	4	0.887	001	7	2	6	8	2	7
3568.2895	2.642E-20	3	0.997	0.418	4	0.896	001	6	2	4	7	2	5
3570.5405	4.383E-21	5	1.006	0.363	8	0.771	001	6	3	4	7	3	5
3576.8506	2.496E-21	8	1.105	0.495	10	1.082	100	5	0	5	5	1	4
3580.0945	3.751E-21	5	1.006	0.260	10	0.672	001	5	5	1	6	5	2
3583.6635	3.490E-21	6	0.977	0.371	9	0.856	100	2	0	2	3	1	3
3586.5430	3.693E-20	3	1.002	0.418	4	0.906	001	6	1	5	7	1	6
3587.7790	4.367E-21	4	0.993	0.322	6	0.870	001	5	4	1	6	4	2
3588.5472	1.310E-20	4	0.993	0.311	5	0.889	001	5	4	2	6	4	3
3593.1974	1.725E-20	4	1.004	0.403	4	0.895	001	5	2	3	6	2	4
3595.3259	2.294E-20	4	0.996	0.382	4	0.924	001	5	3	3	6	3	4
3596.2378	5.506E-21	5	0.989	0.382	7	0.729	100	5	4	2	6	3	3
3599.9951	3.344E-21	7	1.048	0.509	8	1.117	100	2	1	2	2	2	1
3601.0267	6.001E-21	5	1.040	0.448	6	1.207	100	5	3	2	6	2	5
3603.0254	3.561E-21	7	1.065	0.471	10	0.806	100	5	1	4	5	2	3
3606.9935	2.299E-20	4	1.009	0.442	4	1.191	001	5	1	4	6	1	5
3612.5624	5.411E-20	3	1.001	0.425	4	1.145	001	5	2	4	6	2	5
3614.5098	1.455E-20	5	1.010	0.317	4	0.811	001	4	4	0	5	4	1
3614.7024	4.850E-21	5	1.010	0.310	8	0.792	001	4	4	1	5	4	2
3618.0063	6.916E-21	5	1.039	0.490	7	1.128	100	3	0	3	3	1	2
3628.3465	1.134E-19	3	1.007	0.453	3	1.159	001	4	1	3	5	1	4
3629.4467	3.599E-20	3	1.006	0.414	4	1.116	001	5	0	5	6	0	6
3629.6435	1.051E-19	3	1.006	0.413	3	1.113	001	5	1	5	6	1	6
3633.8434	2.953E-20	3	1.003	0.431	4	0.896	001	4	2	3	5	2	4
3638.0820	8.100E-21	4	1.014	0.431	5	0.897	100	1	0	1	1	1	0
3642.5658	5.047E-21	6	1.001	0.386	10	0.761	001	6	0	6	6	2	5
3645.2871	2.757E-21	9	1.005	0.407	15	0.715	001	4	1	3	4	3	2
3646.4636	1.418E-20	3	1.004	0.349	4	0.830	001	3	3	0	4	3	1
3647.5530	4.254E-20	3	1.004	0.380	4	0.921	001	3	3	1	4	3	2
3648.6676	2.074E-21	10	1.000	0.468	12	1.260	100	5	2	3	6	1	6
3649.2830	1.586E-19	3	1.003	0.471	3	1.204	001	4	0	4	5	0	5
3650.6360	5.059E-20	3	1.003	0.446	4	0.909	001	4	1	4	5	1	5
3656.3035	1.101E-19	3	1.007	0.441	3	0.939	001	3	2	2	4	2	3
3670.7496	1.965E-19	3	1.008	0.465	3	0.937	001	3	1	3	4	1	4
3676.0195	1.830E-19	3	1.011	0.427	3	0.904	001	2	1	1	3	1	2
3679.4363	3.135E-20	4	1.006	0.442	4	0.866	001	2	2	1	3	2	2
3680.3735	2.660E-21	8	0.996	0.401	11	0.683	100	2	1	1	2	0	2
3684.5279	4.134E-21	8	1.053	0.471	10	0.805	001	3	0	3	3	2	2
3691.2982	6.816E-20	3	1.006	0.463	3	0.908	001	2	1	2	3	1	3
3696.4624	4.233E-21	7	0.981	0.412	9	0.643	100	5	2	3	5	1	4
3701.7644	8.016E-21	5	1.019	0.486	6	1.181	001	4	1	4	4	1	3
3701.8057	4.871E-20	3	1.023	0.419	3	0.919	001	1	1	0	2	1	1
3709.4023	7.121E-20	3	1.014	0.414	3	0.908	001	1	0	1	2	0	2
3712.2045	1.535E-19	3	1.023	0.511	3	0.952	001	1	1	1	2	1	2
3712.8672	3.505E-21	6	1.117	0.318	11	1.225	001	7	6	2	7	6	1
3714.7943	2.805E-21	5	1.015	0.300	25	0.809	001	6	6	1	6	6	0
3714.7952	8.395E-21	5	1.015	0.145	15	0.579	001	6	6	0	6	6	1
3718.9631	2.128E-20	4	0.992	0.420	4	0.769	001	5	2	4	5	2	3

Table 2 (*continued*)

Wavenumber, cm^{-1}	S_{fit} (cm $molec^{-1}$)	δ (%)	S_{fit}/S [1]	γ^{a}_{fit} (cm^{-1} atm^{-1})	δ (%)	$\gamma^{a}_{fit}/\gamma^{o}$ [1]	V'	J'	Ka′	Kc′	J''	Ka″	Kc″
3722.2222	4.079E-20	3	1.011	0.470	4	0.941	001	3	1	3	3	1	2
3732.1343	1.326E-19	3	1.018	0.435	3	0.906	001	0	0	0	1	0	1
3732.2837	4.902E-21	4	0.996	0.332	6	0.894	001	6	4	3	6	4	2
3734.2726	1.667E-20	4	1.003	0.433	5	0.898	001	4	2	3	4	2	2
3734.6449	1.454E-20	4	0.996	0.326	5	0.893	001	6	4	2	6	4	3
3734.9308	3.831E-20	4	1.009	0.301	4	0.826	001	5	4	2	5	4	1
3735.4447	1.275E-20	4	1.010	0.310	6	0.794	001	5	4	1	5	4	2
3735.4926	2.370E-20	4	1.004	0.384	4	0.879	001	5	3	3	5	3	2
3736.6827	2.967E-20	3	1.010	0.289	4	0.701	001	4	4	1	4	4	0
3736.7433	8.886E-20	3	1.010	0.293	3	0.711	001	4	4	0	4	4	1
3738.4007	2.610E-20	4	1.009	0.448	4	0.891	001	2	1	2	2	1	1
3741.3061	2.205E-20	4	1.006	0.346	4	0.784	001	4	3	2	4	3	1
3743.9465	6.117E-20	3	1.004	0.364	4	0.826	001	4	3	1	4	3	2
3744.5094	1.118E-19	3	1.012	0.431	3	0.891	001	3	2	2	3	2	1
3744.6513	1.790E-19	3	1.011	0.352	3	0.826	001	3	3	1	3	3	0
3745.0868	5.954E-20	3	1.011	0.335	4	0.787	001	3	3	0	3	3	1
3749.3292	1.764E-19	3	1.012	0.427	3	0.863	001	1	1	1	1	1	0
3749.5738	7.968E-20	3	1.013	0.438	3	0.912	001	2	2	1	2	2	0
3752.5007	2.280E-20	4	1.013	0.355	4	0.916	100	4	4	1	4	3	2
3753.8186	7.253E-21	5	1.022	0.397	7	0.702	100	5	4	2	5	3	3
3756.6164	3.665E-20	3	1.005	0.415	4	0.807	001	3	2	1	3	2	2
3759.8445	5.911E-20	3	1.018	0.456	4	0.950	001	1	1	0	1	1	1
3765.7602	4.851E-20	3	1.002	0.444	4	0.904	001	4	2	2	4	2	3
3777.9492	2.639E-21	8	0.984	0.445	11	0.718	100	4	2	3	3	1	2
3779.7622	6.644E-21	6	0.980	0.402	8	0.846	001	5	2	3	5	2	4
3796.4395	5.612E-20	3	1.015	0.506	3	0.942	001	2	1	2	1	1	1
3797.7879	8.478E-21	5	1.030	0.469	7	0.759	001	6	2	4	6	2	5
3807.0136	1.610E-19	3	1.016	0.426	3	0.926	001	2	1	1	1	1	0
3821.7641	1.055E-19	4	1.010	0.463	3	0.926	001	3	2	2	2	2	1
3825.5522	3.092E-21	9	1.004	0.368	14	0.718	100	4	3	1	3	2	2
3826.7539	3.515E-20	4	1.010	0.437	4	0.819	001	3	2	1	2	2	0
3831.6862	7.045E-20	3	1.015	0.405	4	0.818	001	3	1	2	2	1	1
3834.9830	7.520E-20	3	1.013	0.444	4	0.895	001	4	1	4	3	1	3
3837.8693	2.483E-19	3	1.016	0.499	3	1.149	001	4	0	4	3	0	3
3839.9293	1.642E-20	3	1.007	0.372	4	0.899	001	4	3	2	3	3	1
3843.5046	5.616E-21	6	0.960	0.359	11	0.832	001	6	1	5	6	1	6
3843.7507	4.206E-20	3	1.012	0.406	3	0.863	001	4	2	3	3	2	2
3844.8471	2.170E-21	11	0.982	0.426	15	0.737	001	5	3	3	5	1	4
3852.0574	1.949E-19	3	1.013	0.454	3	1.102	001	5	1	5	4	1	4
3853.9662	1.279E-19	3	1.013	0.407	3	0.939	001	4	2	2	3	2	1
3854.0905	6.660E-20	3	1.013	0.452	4	1.097	001	5	0	5	4	0	4
3857.1643	1.822E-20	6	0.980	0.300	4	0.830	001	5	4	2	4	4	1
3857.4250	6.045E-21	6	0.979	0.297	10	0.840	001	5	4	1	4	4	0
3861.7878	4.780E-20	3	1.004	0.361	4	0.872	001	5	3	3	4	3	2
3864.3099	1.123E-20	5	0.980	0.365	7	0.869	001	5	3	2	4	3	1
3865.1115	9.568E-20	3	1.018	0.429	3	0.921	001	5	2	4	4	2	3
3869.1926	4.719E-20	3	1.017	0.392	4	0.880	001	6	1	6	5	1	5
3870.1293	1.428E-19	3	1.017	0.417	3	0.906	001	6	0	6	5	0	5
3873.7244	9.888E-21	4	1.026	0.361	6	0.914	100	5	4	1	4	3	2
3873.9442	7.285E-21	5	0.987	0.341	7	0.821	100	5	4	2	4	3	1
3874.4022	4.739E-20	3	1.013	0.429	3	0.932	001	5	1	4	4	1	3
3879.9495	5.962E-21	4	1.005	0.305	6	0.872	001	6	4	3	5	4	2
3880.1914	3.467E-20	3	1.002	0.373	4	0.906	001	5	2	3	4	2	2
3881.0286	1.785E-20	4	1.006	0.340	5	0.918	001	6	4	2	5	4	1
3883.2666	1.141E-20	5	0.992	0.340	7	0.823	001	6	3	4	5	3	3
3885.6599	9.027E-20	4	1.022	0.351	3	0.946	001	7	1	7	6	1	6
3891.2995	9.016E-20	3	1.016	0.438	3	0.907	001	6	1	5	5	1	4
3892.8270	2.916E-21	7	0.960	0.388	11	0.621	001	3	2	1	2	0	2
3897.9738	2.811E-21	7	0.994	0.340	13	0.757	100	6	4	2	5	3	3
3899.2168	2.839E-20	3	1.053	0.391	4	0.905	001	6	3	3	5	3	2
3899.4413	4.689E-20	3	1.011	0.365	4	0.872	001	7	2	6	6	2	5
3901.6665	1.699E-20	3	1.020	0.319	4	0.862	001	8	1	8	7	1	7
3901.8470	5.100E-20	3	1.020	0.322	4	0.907	001	8	0	8	7	0	7
3902.2500	1.180E-20	7	1.023	0.300	5	0.868	001	7	4	4	6	4	3
3904.1886	6.807E-20	3	1.010	0.412	4	0.915	001	6	2	4	5	2	3
3906.0649	1.672E-20	4	1.004	0.401	4	0.870	001	7	1	6	6	1	5
3916.3287	8.218E-21	3	1.004	0.289	5	0.821	001	8	2	7	7	2	6
3917.2859	2.562E-20	4	0.983	0.261	4	0.843	001	9	1	9	8	1	8
3917.3628	8.526E-21	4	0.983	0.257	7	0.830	001	9	0	9	8	0	8
3920.0887	2.587E-20	3	1.004	0.368	4	0.926	001	8	1	7	7	1	6

Table 2 (*continued*)

Wavenumber, cm^{-1}	S_{fit} (cm $molec^{-1}$)	δ (%)	S_{fit}/S [1]	γ^{s}_{fit} (cm^{-1} atm^{-1})	δ (%)	$\gamma^{s}_{fit}/\gamma^{o}$ [1]	V'	J'	Ka′	Kc′	J''	Ka″	Kc″
3924.3728	4.042E-21	6	1.005	0.290	11	0.798	001	8	3	6	7	3	5
3925.1343	8.201E-21	5	1.117	0.441	6	1.188	001	7	3	4	6	3	3
3925.1758	1.222E-20	4	1.017	0.413	5	1.113	001	7	2	5	6	2	4
3932.1355	1.189E-20	6	1.030	0.291	4	0.875	001	9	2	8	8	2	7
3932.5452	3.889E-21	4	1.004	0.226	8	0.718	001	10	1	10	9	1	9
3932.5806	1.167E-20	4	1.004	0.226	7	0.716	001	10	0	10	9	0	9
3942.6524	1.670E-20	4	1.005	0.399	5	0.910	001	8	2	6	7	2	5
3944.3681	2.764E-21	7	1.043	0.280	12	0.833	001	9	4	6	8	4	5
3947.4632	4.776E-21	5	0.932	0.224	11	0.897	001	11	1	11	10	1	10

* Only those lines are presented whose parameters deviate from the HITRAN-2012 values by more than the error in the derived parameters. The full list of the experimentally derived parameters as compared to the HITRAN-2012 is given in the supplementary file 'Suppl_Tables'.

Acknowledgement

The measurements were made as part of the NERC-EPSRC funded CAVIAR (grant number NE/D012082/1) ("Continuum Absorption at Visible and Infrared wavelengths and its Atmospheric Relevance") consortium, with further analysis during the STFC-funded project "Measuring weak water vapour absorption using a supercontinuum source" (ST/M000281/1). IVP also acknowledges the Russian Program of Fundamental Scientific Investigations II.10.3.8 (Project PhSI no. 01201354620).

Appendix A. Supplementary material

Supplementary data associated with this article can be found in the online version at http://dx.doi.org/10.1016/j.jqsrt.2016.02.001.

References

[1] Rothman LS, Gordon IE, Babikov Yu, Barbe A, Chris Benner D, Bernath PF, Birk M, Bizzocchi L, Boudon V, Brown LR, Campargue A, Champion J-P, Chance K, Cohen EA, Coudert LH, Devi VM, Drouin BJ, Fayt A, Flaud J-M, Gamache RR, Harrison JJ, Hartmann J-M, Hill C, Hodges JT, Jacquemart D, Jolly A, LeRoy RJ, Li G, Long DA, Lyulin OM, Mackie CJ, Massie ST, Mikhailenko SN, Muller HSP, Naumenko OV, Nikitin AV, Orphal J, Perevalov VI, Perrin A, Polovtseva ER, Richard C, Smith MAH, Starikova E, Sung K, Tashkun S, Tennyson J, Toon GC, Tyuterev VlG, Wagner G. The HITRAN2012 molecular spectroscopic database. J Quant Spectrosc Radiat Transf 2013;130:4–50.

[2] Ptashnik IV, Smith KM, Shine KP, Newnham DA. Laboratory measurements of water vapour continuum absorption in spectral region 5000–5600 cm^{-1}: evidence for water dimers. Q J R Meteorol Soc 2004;130:2391–408.

[3] Paynter DJ, Ptashnik IV, Shine KP, Smith KM. Pure water vapour continuum measurements between 3100 and 4400 cm^{-1}: evidence for water dimer absorption in near atmospheric conditions. Geophys Res Lett 2007;34(12):L12808.

[4] Ptashnik IV. Evidence for the contribution of water dimers to the near-IR water vapour self-continuum. J Quant Spectrosc Radiat Transf 2008;109:831–52.

[5] Ptashnik IV, Smith KM, Shine KP. Self-broadened line parameters for water vapour in the spectral region 5000–5600 cm^{-1}. J Mol Spectrosc 2005;232(2):186–201.

[6] Ptashnik IV, Smith KM. Water vapour line intensities and self-broadening coefficients in the 5000–5600 cm^{-1} spectral region. J Quant Spectrosc Radiat Transf 2010;111:1317–27.

[7] Rothman LS, Jacquemart D, Barbe A, Chris Benner D, Birk M, Brown LR, Carleer MR, Chackerian CJr, Chancea K, Couderth LH, Danai V, Devic VM, Flaud JM, Gamache RR, Goldman A, Hartmann JM, Jucks KW, Maki AG, Mandin J-Y, Massie ST, Orphal J, Perrin A, Rinsland CP, Smith MAH, Tennyson J, Tolchenov RN, Toth RA, Vander Auwera J, Varanasi P, Wagner G. The HITRAN 2004 molecular spectroscopic database. J Quant Spectrosc Radiat Transf 2005;96(2):139–204.

[8] Rothman LS, Gordon IE, Barbe A, Chris Benner D, Bernath PF, Birk M, Boudon V M, Brown LR, Campargue A, Champion J-P, Chance K, Coudert LH, Dana V LH, Devi VM, Fally S, Flaud J-M, Gamache RR, Goldman A, Jacquemart D, Kleiner I D, Lacome N, Lafferty WJ, Mandin J-Y, Massie ST, Mikhailenko SN, Miller CE, Moazzen-Ahmadi N, Naumenko OV, Nikitin AV, Orphal J, Perevalov VI, Perrin A, Predoi-Cross A, Rinsland CP, Rotger M, Simeckova M, Smith MAH, Sung K, Tashkun SA, Tennyson J, Toth RA, Vandaele AC, Vander Auwera J. The HITRAN 2008 molecular spectroscopic database. J Quant Spectrosc Radiat Transf 2009;110:533–72.

[9] Mertz L. Auxillary computation for fourier transform spectrometry. Infrared Phys 1967;7:17–23.

[10] Mitsel AA, Ptashnik IV, Firsov KM, Fomin AB. Efficient technique for line-by-line calculating the transmittance of the absorbing atmosphere. Atmos Ocean Opt 1995;8:847–50.

[11] Birk M, Hausamann D, Wagner G, Johns JW. Determination of line strengths by Fourier-transform spectroscopy. Appl Opt 1996;35:2971–85.

[12] Rautian SG, Sobelman II. Effect of collisions on the Doppler broadening of spectral lines. Sov Phys Uspekhi 1967;9:701.

[13] Tennyson J, Bernath PF, Campargue A, Csaszar AG, Daumont L, Gamache RR, Hodges JT, Lisak D, Naumenko OV, Rothman LS, Tran H, Zobov NF, Buldyreva J, Boone CD, Domenica De Vizia M, Gianfrani L, Hartmann JM, McPheat R, Weidmann D, Murray J, Ngo NH, Polyansky OL. Recommended isolated-line profile for representing high-κesolution spectroscopic transitions (IUPAC Technical Report). Pure Appl Chem, 86(12); 2014, p. 1931–43.

[14] (a) Tran H, Ngo NH, Hartmann J-M. Efficient computation of some speed-dependent isolated line profiles. J Quant Spectrosc Radiat Transf 2013;129:199–203;
(b) Tran H, Ngo NH, Hartmann J-M. Erratum to "Efficient computation of some speed-dependent isolated line profiles [J. Quant. Spectrosc. Radiat. Transfer 129 (2013) 199-203]. J Quant Spectrosc Radiat Transf 2014;134:104.

[15] Kochanov VP. Line profiles for the description of line mixing, narrowing, and dependence of relaxation constants on speed. J Quant Spectrosc Radiat Transf 2011;112:1931–41.

[16] Nelkin M, Ghatak A. Simple binary collision model for Van Hove's G_s(r,t). Phys Rev 1964;135(1A):A4–9.

[17] Brown LR, Chris Benner DC, Devi VM, Smith MAH, Toth RA. Line mixing in self- and foreign-broadened water vapor at 6 μm. J Molec Struct 2005;742:111–22.

[18] Polyansky OL, Kyuberis AA, Zobov NF, Tennyson J, Lodi L. Calculation of complete water linelist up to dissociation. Mon Not R Astron Soc 2016 [in prepration].

[19] Tennyson J, Kostin MA, Barletta P, Harris GJ, Polyansky OL, Ramanlal J, Zobov NF. DVR3D: a program suite for the calculation of rotation–vibration spectra of triatomic molecules. Comput Phys Commun 2004;163(2):85–116.

[20] Lodi L, Tennyson J, Polyansky OL. A global, high accuracy ab initio dipole moment surface for the electronic ground state of the water molecule. J Chem Phys 2011;135:034113–110.

[21] Bubukina II OL, Zobov NF, Polyansky OL, Shirin SV, Yurchenko SN. Optimized semiempirical potential energy surface for $H_2^{16}O$ up to 26000 cm^{-1}. Opt Spectrosc 2011;110:160–6.

[22] Lisak D, Havey DK, Hodges JT. Spectroscopic line parameters of water vapor for rotation-vibration transitions near 7180 cm^{-1}. Phys Rev A 2009;79:052507.
[23] Pogany A, Klein A, Ebert V. Measurement of water vapor line strengths in the 1.4–2.7 μm range by tunable diode laser absorption spectroscopy. J Quant Spectrosc Radiat Transf 2015;165:108–22.
[24] Toth RA, Brown LR, Plymate C. Self-broadened widths and frequency shifts of water vapor lines between 590 and 2400 cm^{-1}. J Quant Spectrosc Radiat Transf 1998;59:529–62.
[25] Toth RA. Linelist of water vapor parameters from 500 to 8000 cm^{-1}, measured values, see ⟨http://mark4sun.jpl.nasa.gov/data/spec/H2O⟩.
[26] Toth RA. Linelist of water vapor parameters from 500 to 8000 cm^{-1}, see ⟨http://mark4sun.jpl.nasa.gov/h2o.html⟩.
[27] Coudert LH, Wagner G, Birk M, Baranov YI, Lafferty WJ, Flaud J-M. The $H_2^{16}O$ molecule: line position and line intensity analyses up to the second triad. J Mol Spectrosc 2008;251:339–57.
[28] Martin MA, Coudert L, Pirali O, Balcon O. Intensities of water vapor transitions in 0–6000 cm^{-1} region. J Chem Phys 2016 [in preparation].
[29] Gamache RR, Hartmann J-M. An intercomparison of measured pressure-broadening and pressure-shifting parameters of water vapour. Can J Chem 2004;82:1013–27.
[30] Antony BK, Gamache RR. Self-broadened half-widths and self-induced line shifts for water vapor transitions in the 3.2–17.76 μm spectral region via complex Robert-Bonamy theory. J Mol Spectrosc 2007;243:113–23.
[31] Birk M, Wagner G. Temperature-dependent air-broadening of water in the 1250–1750 cm^{-1} range. J Quant Spectrosc Radiat Transf 2012;113:889–928.
[32] Mandin J-Y, Camy-Peyret C, Flaud J-M, Guelachvili G. Measurements and calculations of self-broadening coefficients of lines belonging to the $2\nu2$, $\nu1$, and $\nu3$ bands of $H_2^{16}O$. Can J Phys 1982;60:94–101.
[33] Rothman LS, Gordon IE, Barber RJ, Dothe H, Gamache RR, Goldman A, Perevalov VI, Tashkun SA, Tennyson J. HITEMP, the high-temperature molecular spectroscopic database. J Quant Spectrosc Radiat Transf 2010;111:2139–50.
[34] Toth RA. Measurements and analysis (using empirical functions for widths) of air- and self-broadening parameters of H_2O. J Quant Spectrosc Radiat Transf 2005;94:1–50.
[35] Rothman LS, Barbe A, Chris Benner D, Brown LR, Camy-Peyret C, Carleer MR, Chance K, Clerbaux C, Dana V C, Devi VM, Fayt A, Flaud J-M, Gamache RR, Goldman A, Jacquemart D, Jucks KW, Lafferty WJ, Mandin J-Y, Massie ST, Nemtchinov V ST, Newnham DA, Perrin A, Rinsland CP, Schroeder J, Smith KM, Smith MAH, Tang K, Toth RA, Vander Auwera J, Varanasi P, Yoshino K. The HITRAN molecular spectroscopic database: edition of 2000 including updates through 2001. J Quant Spectrosc Radiat Transf 2003;82:5–44.